UNCLASSIFIED

Australian Government

Department of Defence

Science and Technology

Radar Detection of Helicopters at low SNR using Time-Frequency Transforms

Duong Duc Nguyen[1], *Si Tran Nguyen Nguyen*[2], *Rocco Melino*[2], *Sandun Kodituwakku*[2] *and Hai-Tan Tran*[2]

[1] **The University of Adelaide**

[2] **National Security and ISR Division**

Defence Science and Technology Group

DST-Group–TR–3481

ABSTRACT

This report describes a radar signal processing technique for detecting helicopter targets based on the micro-Doppler components of the received signal, in a low SNR environment. The Short-Time Fourier Transform (STFT) and the tunable Q-factor wavelet transform were used to identify the micro-Doppler components induced from the rotating main and tail rotor blades of a helicopter radar return. The impact of the STFT parameters on identifying the blade-like components in the reflected signal was investigated. A strong correlation exists between the STFT parameters and the physical properties of the main and tail rotor blades, which can be used to tune the algorithm and improve the detection performance. The algorithms proposed are demonstrated using measured radar data from two different helicopter types.

RELEASE LIMITATION

Approved for Public Release

UNCLASSIFIED

Published by

National Security and ISR Division
Defence Science and Technology Group
PO Box 1500
Edinburgh, South Australia 5111, Australia

Telephone: 1300 333 362
Facsimile: (08) 7389 6567

AR-017-169
April, 2018

Radar Detection of Helicopters at low SNR using Time-Frequency Transforms

Executive Summary

This report contains a technique for detecting helicopter targets in radar returns in low signal to noise ratio (SNR) scenarios. In most cases the fuselage return from an airborne target produces the strongest Doppler spectral component, making radar target detection from its body return alone easily achievable. However, this does not provide any additional information regarding the type of target observed. For example, slow moving helicopters can be mistaken for other low speed targets such as ground moving vehicles. By exploiting the micro-Doppler characteristics of the helicopter's radar return caused by its rotating main and tail rotor blades, the detection of the blade-like components in the signal can be used for identifying helicopter targets.

In this work, we take advantage of micro-Doppler characteristics of the target and use the Short-Time Fourier Transform (STFT) to detect rotor blade returns in the received signal. By optimising the STFT parameters, helicopter targets can be detected in returns with a low SNR.

Our proposed algorithm was applied to measured data featuring two helicopter types, namely the Bell 206 and Squirrel AS350. For both helicopter types, the main rotor blades can be detected with a probability of 0.6 at SNR levels as low as -24 dB using a coherent processing interval (CPI) of 150 ms and using the STFT parameters that are matched to the temporal characteristics of the main rotor blade. Once detected, the main blade can be coherently separated from the received signal, and tail rotor blade detection can be subsequently performed. The success of the tail rotor blade detection depends on its SNR level, and the orientation of the helicopter relative to the radar line-of-sight. By using this blade detection process for both main and tail rotors, coarse classification of helicopter targets is possible.

This page is intentionally blank

Authors

Mr Duong Duc Nguyen
The University of Adelaide

Duong Duc Nguyen received his Bachelor of Science degree in Electronic Communication Systems from University of Plymouth and his M.Sc. degree in Mobile and Personal Communications from King's College London, United Kingdom, in 2008 and 2009, respectively. He is currently working towards the PhD degree at the School of Electrical and Electronic Engineering, the University of Adelaide. His research interests include signal processing and reinforcement learning techniques for emerging future networks.

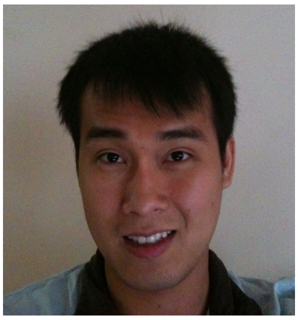

Dr Si Tran Nguyen
National Security and ISR Division

Si Tran Nguyen graduated from the University of Adelaide in 2007 and worked for Codan Limited, South Australia as a microwave graduate engineer in the following year. In 2014, he obtained his PhD from the University of Adelaide in signal processing. From 2012 to 2017, he worked with the University of Adelaide Radar Research Centre on various projects in collaboration with the Australia Bureau of Meteorology and Defence Science and Technology (DST) Group. He is now with the National Security and ISR Division of DST Group. His research interests include rational rate filter banks, rational wavelet transforms, sparse signal representation, and radar signal processing.

Mr Rocco Melino
National Security and ISR Division

Rocco Melino received a Bachelor Degree in Electronic Engineering from the University of South Australia in 1999 and received his Masters Degree in Signal and Information Processing from the University of Adelaide in 2010. He has been working for the National Security and ISR Division of DST Group since 1999. His research interests include radar automatic target recognition, radar modelling and high resolution radar imaging.

Dr Sandun Kodituwakku
National Security and ISR Division

Sandun Kodituwakku received a Bachelor of Engineering (Electrical and Electronic) with first class honours from the University of Adelaide in 2006, and a PhD in signal processing from the Australian National University in 2012. He works as a radar signal processing specialist in the National Security and ISR Division of DST Group since 2011. His research interests include radar detection, adaptive signal processing, compressive sensing, automatic target recognition, radar imaging, and various topics in radar signal processing.

Dr Hai-Tan Tran
National Security and ISR Division

Hai-Tan Tran graduated from the University of Sydney in 1990 and obtained his PhD degree from the Australian National University in Canberra in 1993, in the field of nonlinear guided-wave optics. He spent the next three years as a postdoctoral research fellow in the Mathematics Department of the Australian Defence Force Academy, also in Canberra, working on the theory and simulation of spatial optical solitons and light-induced optical switching in nonlinear dielectric media, before joining the National Security and ISR Division of DST Group in 1996. His current research interests include high-resolution radar imaging, automatic target recognition, compressive sensing, and various topics in advanced signal processing.

Contents

Figures

Tables

This page is intentionally blank

1. Introduction

In this report, we present a radar signal processing algorithm for detecting helicopters from the micro-Doppler returns induced from the rotating rotor blades in the presence of noise. These micro-Doppler returns from the main and tail rotor blades exhibit unique temporal and spectral characteristics which allow them to be distinguished, using time-frequency analysis, from other components in the radar return such as the helicopter fuselage.

In most cases the fuselage return from a helicopter is the dominant component in the radar return, making radar target detection from the fuselage return easily achievable [1, 2, 3]. However, for slow-moving helicopters where the body Doppler frequency is close to 0 Hz, a helicopter return can be buried in the clutter or can be misidentified for another low speed target, such as a ground moving vehicle. Hence, the detection of micro-Doppler components in the signal can be useful for specifically detecting helicopters and can lead to coarse target classification [4].

In our previous work [5, 6, 7], separation of the rotor blade components based on a sparse signal representation and the wavelet transform was discussed and verified with measured radar data of helicopters where the received signal had a high signal-to-noise ratio (SNR). Stationary and non-stationary spectral characteristics were modelled using the Tunable Q-factor Wavelet Transform (TQWT), and a Basis Pursuit De-noising (BPD) optimisation technique was used to reconstruct micro-Doppler signals of interest. In this report, these techniques are used to demonstrate the radar detection of helicopter micro-Doppler components, such as those induced from the rotating rotor blades, in the more challenging low SNR environment.

In the time domain, returns from the main and tail blades have regularly spaced *spikes*, known as blade flashes. After filtering out low-frequency terms, the blade flashes in the time-domain can be detected. Misiurewicz et al. [8] used a constant-false alarm rate (CFAR) system with a detection threshold of 14 dB above the noise level to detect blade flashes with a very low false alarm rate, but the method relies on high SNR. In the Doppler domain, the helicopter returns are distributed across the spectrum, and consist of the fuselage return (which will be close to 0 Hz for a hovering helicopter), the low frequency rotor hub return, and the flat plateau returns from the main blade whose Doppler frequency extends from the centre of rotation to the blade tip [2, 4]. Misiurewicz [4, 8] proposed methods to detect these components in the spectral domain using a geometric model based approach. The time and frequency domain analysis of helicopter returns can yield good detection results, however it degrades rapidly in the presence of noise and clutter.

Using time-frequency analysis, the frequency response of a signal can be tracked over time. A number of techniques for helicopter micro-Doppler signal analysis in the combined temporal and spectral domains have been proposed in the literature [2, 9, 7], making this the most widely used class of technique for analysing radar micro-Doppler signatures. Chen et al. [2] discussed the use of different time-frequency analysis methods, such as the linear short-time Fourier transform, nonlinear transforms such as Wigner-Ville and Choi-Williams, and adaptive time-frequency transforms to investigate the micro-Doppler signals resulting from rotating targets, such as those from helicopter main and tail rotor blades. The aim was to separate the micro-

Doppler signal components from the zero Doppler components of a target. From the extracted micro-Doppler signatures, information about target dynamics and structural composition can be estimated, which is critical for target identification. In [7], a sparse representation and the wavelet transform were used to detect blade-like components in the signal by exploiting their unique temporal and spectral characteristics.

Haghshenas [10] proposed an amplitude and phase demodulation (AM and PM) technique to model helicopter rotor returns, and used this as the basis for helicopter detection. However, a high SNR is required for the AM demodulation model to work accurately. Helicopter detection was not only investigated in the context of active radar, but also has been considered in the passive radar context with digital video broadcasting (DVB-T) as an illuminator of opportunity [3]. Additionally, Gini proposed a matched subspace CFAR detection method for detecting hovering helicopters [11].

The acoustic signature of helicopters has also been used for detection of helicopters [12, 13]. These methods utilise the ratio of main and tail rotor fundamental audio frequencies of the helicopter acoustic signature, and use a look-up table to identify the helicopter. These methods rely on measuring both the main and tail rotor audio frequencies at the receiver. However, this technique cannot be used for long range detection and performs poorly due to attenuation caused by the helicopter's orientation or poor atmospheric conditions. A more advanced detection method of helicopters using their acoustic signatures based on artificial neural networks (ANN) is proposed in [14, 15]. ANN detectors were trained using recorded audio from real helicopters in conjunction with audio from a number of non-helicopter sources. Again, the detection ranges are limited due to an inability to capture audio with good SNR.

Another approach for detecting helicopters was based on analysing high resolution radar images [16, 17]. This approach uses image processing techniques, such as the Hough transform [16], for the detection of target boundaries in the image space, which is then converted to the peak detection in the parameter space. The major drawback of this approach is that a wideband radar is required for obtaining the desired high resolution image, and the technique requires high computational complexity.

The work in this report builds on our previous work in [7], where a blade flash detection algorithm based on the STFT and TQWT was used to detect helicopter targets. Here, we evaluate the impact of varying several critical parameters such as the STFT window-size, overlap factor, and the coherent processing interval (CPI) on the detection of non-stationary blade flash returns in the composite radar return. We provide optimal ranges for tuning these parameters to improve the detection of helicopters in low SNR conditions.

2. Blade Flash Detection

In [7], a blade flash detection algorithm was discussed which used the STFT followed by the projection of the time-frequency space onto the time axis. The maximum term of the projected signal was further processed with its Q-factor[1] used as a metric to declare a blade flash detection. This method was part of the automatic blade flash signal separation algorithm.

[1] Q-factor is defined as the ratio between the carrier frequency and signal bandwidth.

In this section we will outline the detection algorithm and describe the measured data used to demonstrate the proposed technique.

2.1. Data Description

The measured data was collected during dedicated helicopter trials held in May 2011. The Defence Science and Technology (DST) Group's Wandana II van-mounted experimental pulse Doppler radar was used to illuminate Bell 206 and Squirrel AS350 helicopters. For each helicopter, datasets were collected while the helicopters were hovering at various aspect angles with respect to the radar. The radar collected measurements at a carrier frequency of 9.5 GHz (X-band) using a PRF of 66.7 kHz with horizontal polarisation on transmit and receive. A single sample per pulse of the radar return was collected. Figure 1 is a plot of the STFT of Bell and Squirrel helicopter data, showing main and tail blade returns.

2.2. Algorithm Description

Blade flash detection involves

1. pre-processing the signal to remove unwanted components,
2. identifying the blade flashes, and
3. declaring a detection based on a Q-factor threshold.

First, pre-processing of the time signal is performed, which involves shifting the helicopters body Doppler return to 0 Hz, followed by DC filtering to remove this dominant component. This is followed by a hub Doppler estimation process, which is described in Section 3.1.2 of [7]. From here, the strong hub returns in the low frequency region are nulled (set to zero) so that they will not interfere with the blade-flash signal. What remains in the composite signal are main and tail blade components. Using the signal separation technique described in [7], the main-blade component is extracted. A blade flash detection is declared based on the Q-factor of this signal.

The noise level is estimated and the time-frequency image is re-scaled by subtracting the estimated noise power from the STFT (Figure 2a). Thus, each data point of the scaled STFT represents the SNR and hence the region dominated by noise can be observed. Figure 2a represents a typical STFT SNR plot with x-axis representing slow-time and y-axis representing the frequency (Doppler) domain.

As illustrated in Figure 2a, the response from both main and tail rotor blades can be clearly observed in this high SNR case. It is expected that the non-stationary blade flashes exhibit a spectrum where most of the energy is concentrated in a very small time interval (this time support is associated with the rotation rate of the blade of interest), spread over a broad Doppler frequency extent. Thus, for automatic detection of such a component, a projection to the time-axis or Radon transform at 0°orientation is applied to the STFT in Figure 2a. This is done by computing a summation of the pixel's intensity for each column of the image.

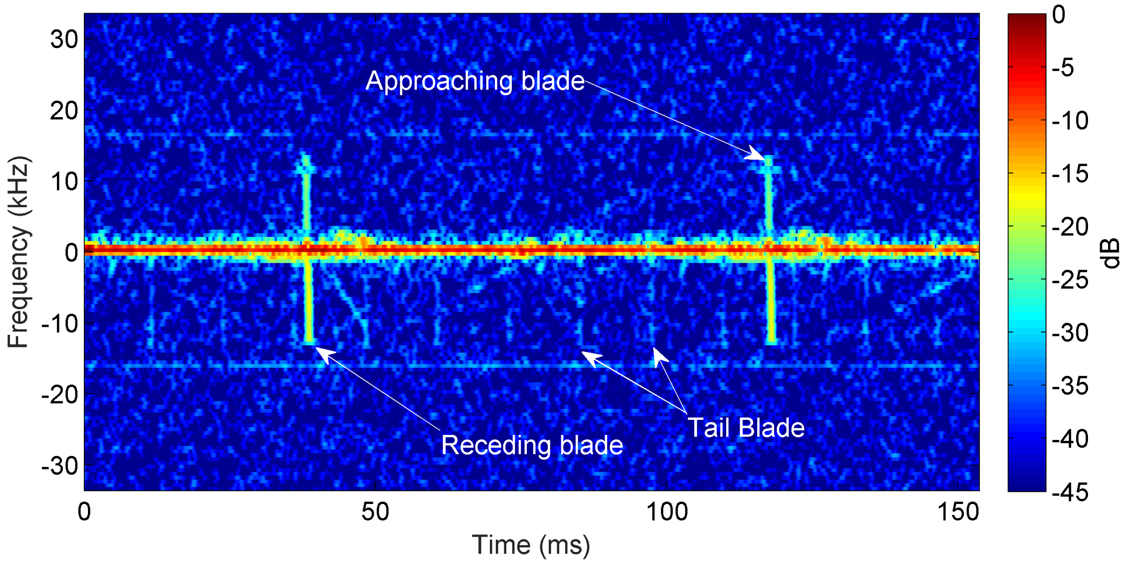

(a) Plot of the STFT of radar data from a Bell helicopter (2 rotor blades)

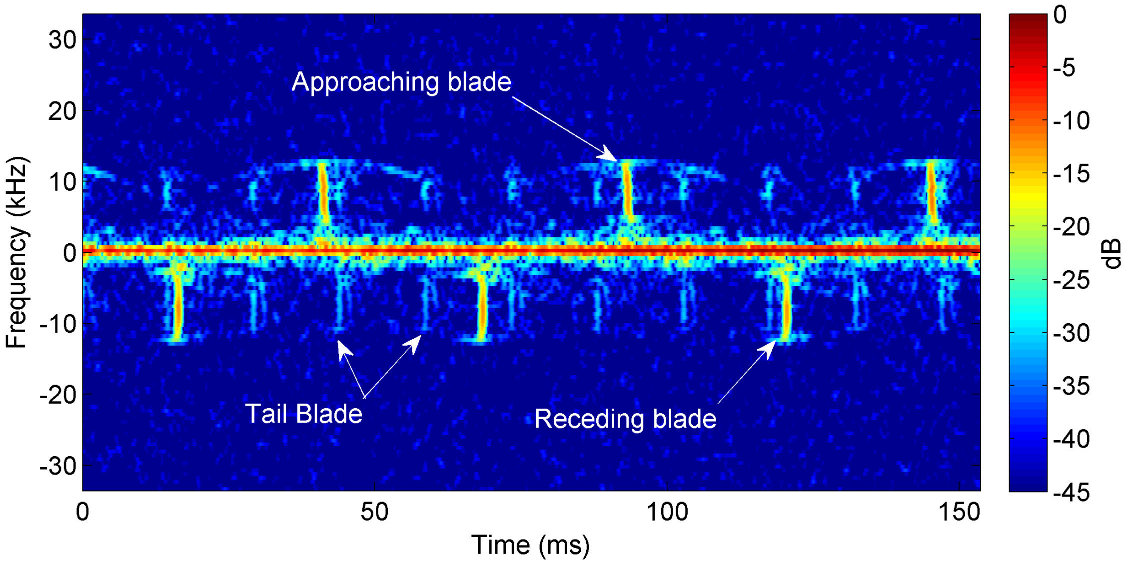

(b) Plot of the STFT of radar data from a Squirrel helicopter (3 rotor blades)

Figure 1: STFT plots of the radar data from Bell and Squirrel helicopters showing the high amplitude fuselage return at 0Hz and the main and tail blade returns.

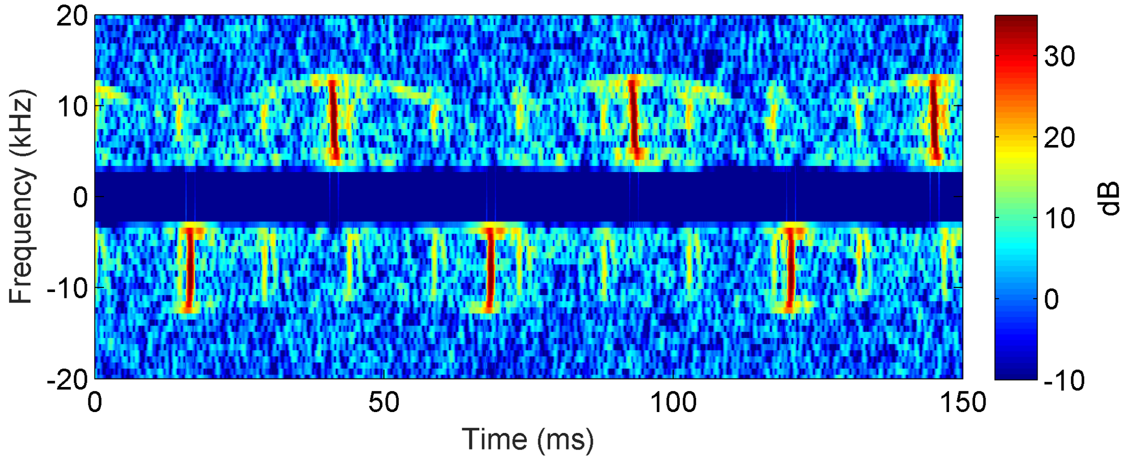

(a)

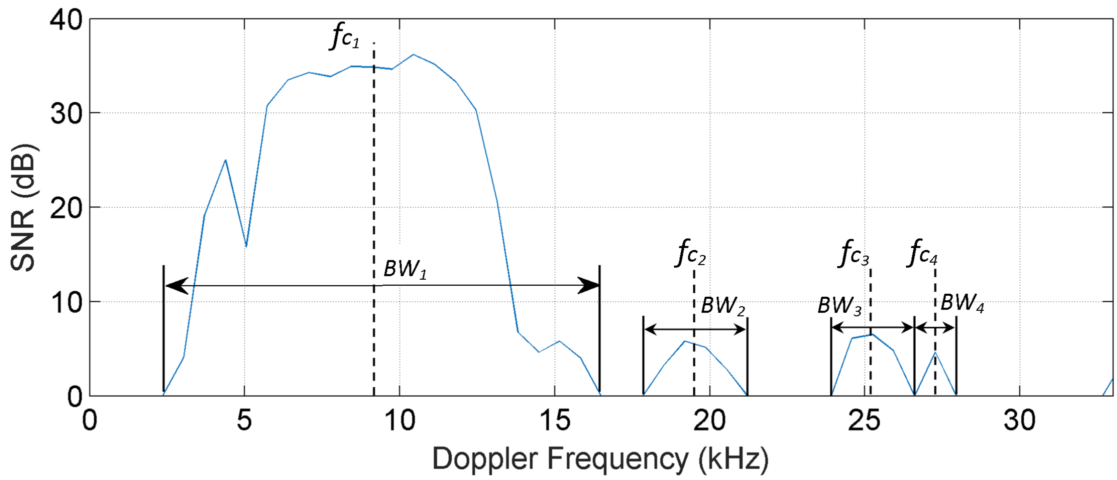

(b)

Figure 2: a) A typical STFT plot of the Squirrel helicopter signal (X-band, 45° aspect angle), normalised to the noise level. The hub Doppler region has been set to $-\infty$ dB, b) Spectrum of the strongest approaching blade flash, detected at τ_p, showing the extent of the contiguous frequency response.

It should be noted that the projection is computed for the positive and negative sides of the spectrum separately. The results of the projection yields a one dimensional measure of power versus time. The time instance of the maximum term in the projection for both positive and negative sides of the spectrum are respectively denoted τ_p, τ_n. These represent the two time values of the strongest approaching and receding blades.

The next step is to declare whether a blade flash exists. First, the spectra of the signals at τ_p, τ_n are considered. These are the columns of the two-dimensional STFT in Figure 2a at the time indices associated with τ_p, τ_n. Next, a threshold of 3dB SNR is applied to remove the frequency bins whose power falls below this threshold, resulting in the thresholded positive blade flash spectrum as illustrated in Figure 2b. The algorithm then finds the starting and ending frequencies where the spectrum has non-zero terms. This Doppler frequency extent is denoted as the bandwidth (BW), which depends on the SNR and different to the conventional definition of some amounts of dBs from the peak. For example in Figure 2b, four BW components are found. The algorithm computes the Q-factors of each component defined as f_c/BW, where f_c is the frequency in the centre of BW.

The blade flash component is non-stationary, with a broad Doppler characteristic. Thus, it is expected that the blade flash has a low Q-factor. Here, we rely on Q-factor to distinguish between the blade flash and other point scatterer targets which exhibit a narrowband Doppler characteristic (for a short CPI, point scatterers Doppler frequencies are approximately constant).

If the Q-factor computed for all the components in the spectrum falls below a predefined threshold, the signal is considered to contain a blade flash component. The pre-defined Q-factor threshold for this report is 1.5, and is selected empirically and based on a large number of datasets analysed. If a blade flash is not detected (Q-factors calculated are greater than 1.5), the algorithm exits, indicating there is no blade flash in the signal. For the example in Figure 2b, a blade signal is detected since the first component has a contiguous frequency ranging from approximately 3 kHz to 16 kHz (BW 13kHz) and has an approximate centre frequency of 9 kHz, making its Q-factor less than the 1.5.

It should be noted that the performance of the detection algorithm relies on the intensity difference (or contrast) between the blade flash components and interfering components in the STFT image in Figure 2a. To ensure this difference is maximised the optimal STFT parameters must be selected. The window-size and overlapping factor can be determined from the physical properties of the rotor blades of interest such as the blade rotation rate. In the scenario where the signal has a high SNR, the blade flash signal can be easily observed and detected, and the STFT parameter selection is not critical. The following section investigates the detection performance with respect to a change in blade flash SNR and STFT parameters.

3. Filter Parameters for Optimal Blade Detection

The parameters used in the detection algorithm are: 1) the FFT window size, overlapping factor and CPI, which are the STFT parameters, and 2) the Q-factor threshold. This section investigates the impact of the STFT parameters on blade detection and discusses the relationship between these parameters and the physical parameters of the blade of interest, such as the rotation rate and blade length. The impact is quantified by presenting detection performance in varying noise using measured data. The noise is artificially generated and added to the real measured data to generate various SNR levels.

To measure algorithm performance, we say a correct detection has occurred when the algorithm identifies a blade flash component that corresponds to the real time instance of the actual blade flash, which is known within ± 0.6 ms.

3.1. Impact of STFT window-size

In this section, we present our findings of how different values of the STFT window-size, denoted as n_s, could impact the performance of the blade detection algorithm. To investigate this, various values in the interval $n_s \in [0.4, 4]$ ms, will be considered. For each value of n_s, the probability of detection is computed using the criterion stated earlier. Here, the CPI is set to 150 ms and the overlap factor is set to 50%.

To measure the probability of detection, artificial white Gaussian noise of various levels is added to the original measured data using the method described in Section IV.C of [5]. For each noise level, 100 realisations are generated. The signal with noise added will be used to compute the estimated time indices of the blade flash using the proposed detection algorithm. Thus, the probability of detection for each noise level is determined by the number of detections divided by 100. The analysis is performed on measured data presented in the next sections.

3.1.1. Bell Helicopter

We first report our empirical results on the Bell helicopter. The dataset used in this case study was measured while the Bell helicopter was hovering with 180°aspect with respect to the radar, or when the helicopter was 'tail on'. Additive noise is applied to the original measured data after the DC filtering stage to vary the SNR from -36 dB to 0 dB. The SNR is defined as the extracted main blade signal power to added complex Gaussian noise averaged over a full cycle of blade rotation. The instantaneous SNR of the flash is large, and can be hard to compute consistently, thus the average SNR for a full rotation of the blade is used in this report. Figure 3 shows the STFT of the DC filtered Bell helicopter return with added noise at SNR $= -24$ dB. Compared to the STFT in Figure 1a, blade flash features are hard to see in this high noise environment.

We then measure the probability of detection for different values of the STFT window-size. Figure 4 shows the impact of the STFT window-size on detecting the main blade signal. We observe that peak detection performance occurs at $n_s \in [0.4, 1]$ ms, as shown in Figure 4. This result implies that when a longer window-size is used, more noise energy is captured, and a shorter window-size degrades the Doppler resolution in the STFT therefore reducing the observed SNR.

To determine an optimal range of the STFT window-size for the detection algorithm in low

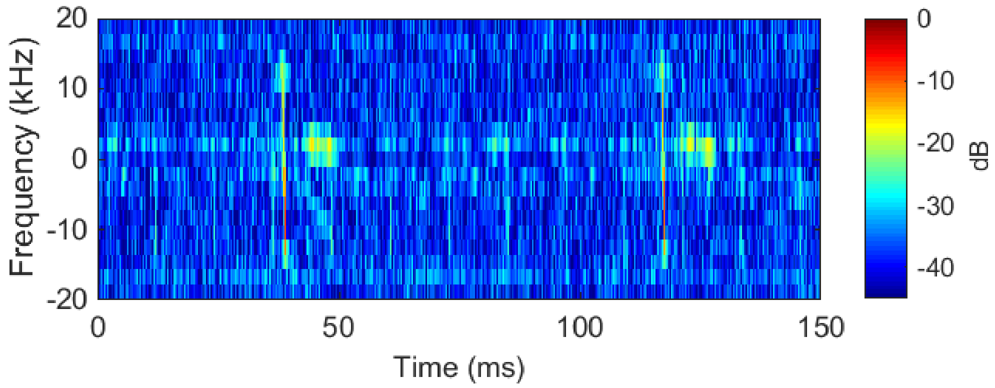

Figure 3: Spectrogram of Bell helicopter returns with added noise at SNR= −24 dB.

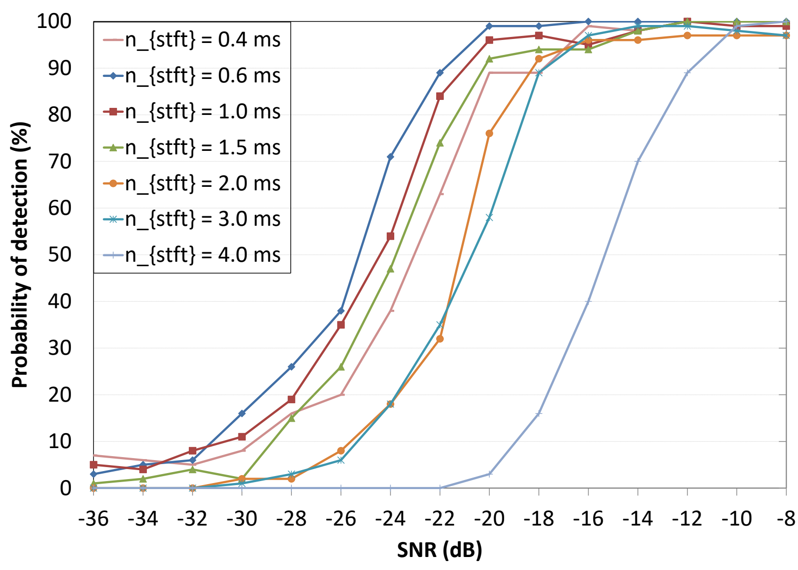

Figure 4: The probability of detection versus the SNR of the main rotor blade signals for hovering Bell helicopter at 180° aspect angle.

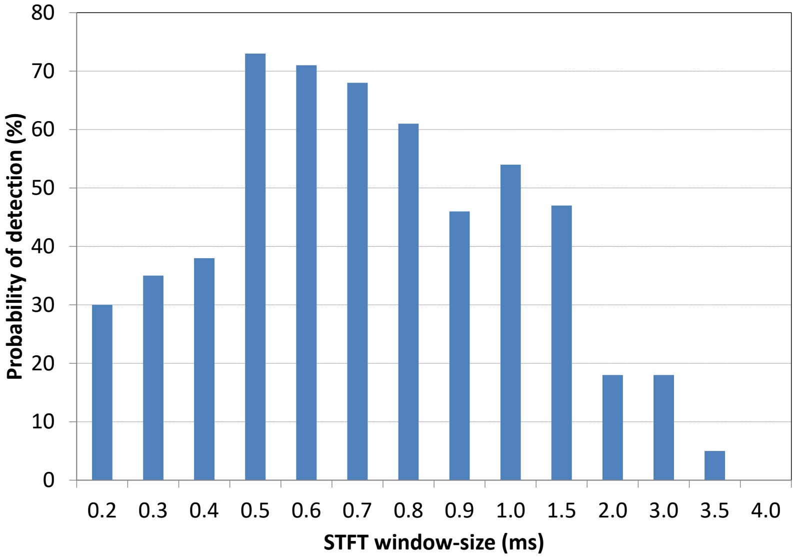

Figure 5: The probability of detection versus the STFT window-size for hovering Bell helicopter at 180° aspect, with SNR is at -24 dB.

SNR conditions, we now fix the SNR level of the main rotor blade signal at -24 dB which gives a wide dynamic range of P_d values as per Figure 4, and vary the STFT window-size from 0.2 ms to 4 ms. Figure 5 shows the algorithm performance versus the STFT window-size of the Bell helicopter when the SNR of the main rotor blade signal is at -24 dB. The optimal range of the STFT window-size to achieve good detection performance is from 0.5 ms to 1.0 ms. This confirms our finding about the impact of the STFT window-size on the performance of the detection algorithm as discussed previously.

To demonstrate the STFT window-size on the blade flash detection for the Bell measurements, Figure 6 shows the original time-domain signal with no noise added, plotted with the STFT time-domain projection with a SNR = -24 dB for $n_s = 2.5$ ms and $n_s = 0.5$ ms. For the longer n_s, the maximum term in the time-domain projection doesn't correspond with a blade flash. However, using $n_s = 0.5$ ms, the maximum component in the time-domain projection corresponds with the time-domain blade flash giving a correct detection.

3.1.2. Squirrel Helicopter

A similar investigation to show the impact of the STFT window-size on the detection algorithm was performed for the Squirrel helicopter. The dataset used in this case was measured while the helicopter was hovering at 0° aspect with respect to the radar, or when the helicopter was 'nose on'. Figure 7 illustrates the impact of the STFT window-size on detecting the main blade signals. Again, the detection performance is best for $n_s = 0.6$ ms and degrades for increasing values of n_s.

Figure 8 shows the algorithm performance versus the STFT window-size when the SNR of the main blade signal is set to -18 dB. The optimal range of n_s for this dataset is $0.6 - 0.9$ ms. Figure 9 shows the original time-domain signal with no noise added and the time-domain

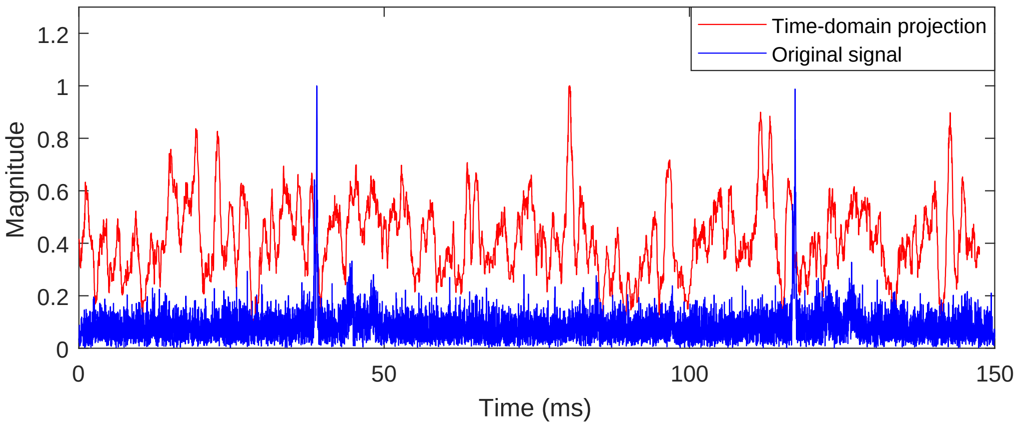

(a) Using $n_s = 2.5ms$

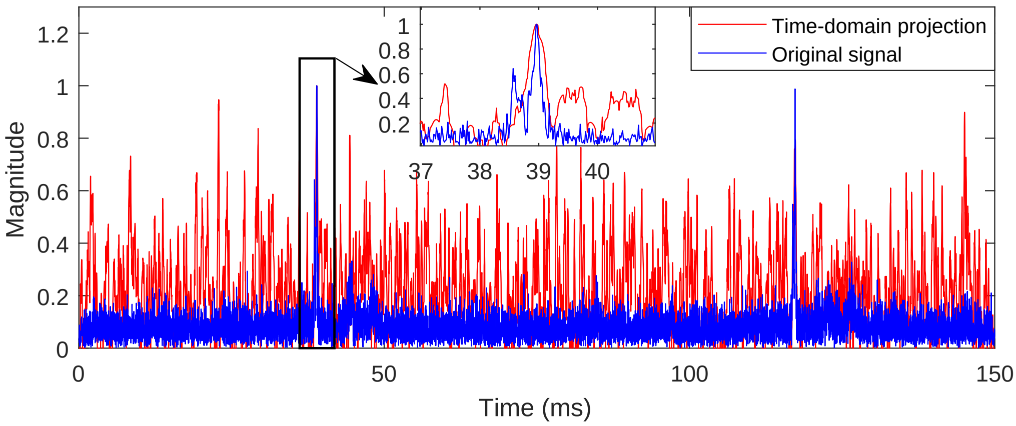

(b) Using $n_s = 0.5ms$

Figure 6: The original signal (no added noise) and time-domain Radon transform projected signal with a $SNR = -24$ dB, for the Bell helicopter measured at 180° aspect.

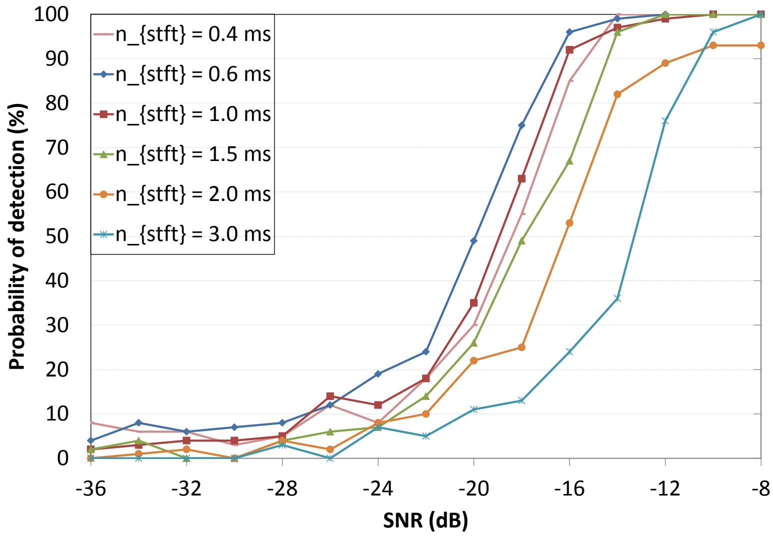

Figure 7: The probability of detection versus the SNR of the main rotor blade signals for hovering Squirrel helicopter at 0° aspect angle, calculated using varying values of n_s.

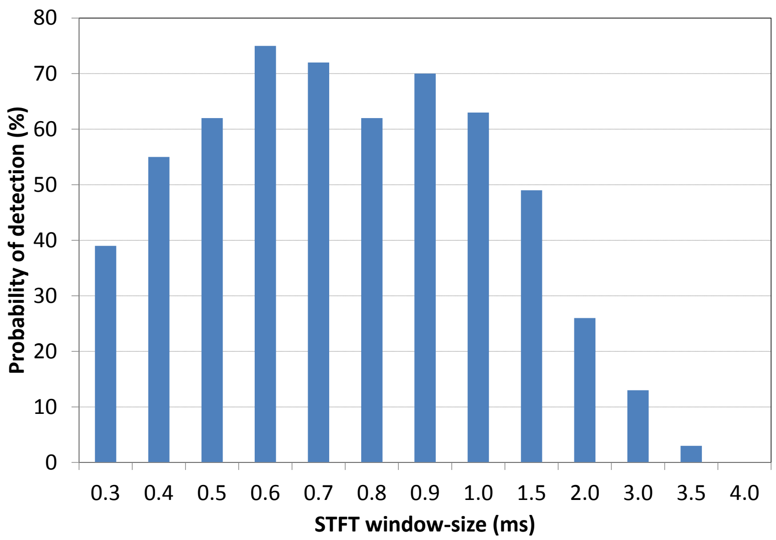

Figure 8: The probability of detection versus the STFT window-size for hovering Squirrel helicopter at 0° aspect, with the SNR $= -18dB$, calculated using varying values of n_s.

projection for the Squirrel measurements made at 0° aspect. Again, the maximum term in the projection corresponds with the blade flash in the time-domain when $n_s = 0.6$ ms, giving a correct detection.

3.1.3. Theoretical Explanation of Experimental Results

To explain the observations seen in the two datasets, we can resort to an important parameter for detection, namely the radar cross-section [1], which directly impacts the amount of energy that is reflected back to the radar. As was presented in Chapter 5 of [1], a main rotor blade modelled as a rectangular plate of length L, has a radar cross-section (RCS), σ, given as

$$\sigma = A \ \operatorname{sinc}^2\left(\frac{2\pi L}{\lambda}\sin\theta\right)\cos^2\theta, \tag{1}$$

where $\operatorname{sinc}(x) = \sin(x)/x$, A is a multiplicative constant dependant on electrical properties of the blade material, λ is the wavelength of the transmitted signal, and θ is the incident angle relative to the normal direction of the rectangular plate, referred to as the 'look angle' of the radar (see Figure 10). Also, using the parameters for the Bell helicopter dateset where the blade length is approximately 5m and $\lambda = 0.0316$ m, the 3dB main-lobe width is $\frac{0.44\lambda}{L} = 0.16°$ and is $\frac{\lambda}{L} = 0.36°$ between nulls. A plot of σ as a function of θ is shown in Figure 11.

From Equation (1), the RCS follows a $\operatorname{sinc}^2(\cdot)$ function multiplied by $\cos^2\theta$ factor, implying the blades RCS peaks at $\theta = 0°$ (broadside aspect) and rapidly falls off for larger angles, as seen in Figure 11. Since the optimum window-size for detection is approximately 0.5 ms and the angular position is $\theta = \omega t$, (where $\omega = 41$ rad/s is the rotation rate), the angular extent of the STFT window is 1.2°. By looking at Figure 11, the optimum STFT window-size covers the main-lobe plus several side-lobes of the RCS response suggesting that this is the compromise between blade signal and noise. That is, if the window-size is too long then more noise is captured compared to blade energy, and if the window-size is too short, not enough of the blade energy is captured.

3.2. Impact of CPI

In this section, we investigate the impact of varying the coherent processing interval (CPI) on the detection of non-stationary blade returns in the composite radar return using short CPI values where less than a full rotation of the rotor is observed. We run the simulation for two cases: Bell helicopter at 180° aspect and Squirrel helicopter at 0° aspect. The results are presented in Tables 1 and 2 respectively, and should be read in conjunction with the STFT plots in Figure 1.

Table 1 presents the main blade measured Q-factor and time values (τ) for approaching and receding blades (±ve) for varying CPI values for the Bell helicopter. The estimated Q-factor for the approaching and receding blades using a CPI of 50 ms is 0.5. This is below the Q-factor detection threshold of 1.5 and hence a main blade is detected on both sides of the spectrum. The maximum blade flashes were detected at 38.7 ms and 39.1 ms for the approaching and receding blades respectively. Using a CPI of 75 ms, the same blade flashes were detected and hence detection was also declared. The τ values in the table correspond with the main blade flashes seen in Figure 1a.

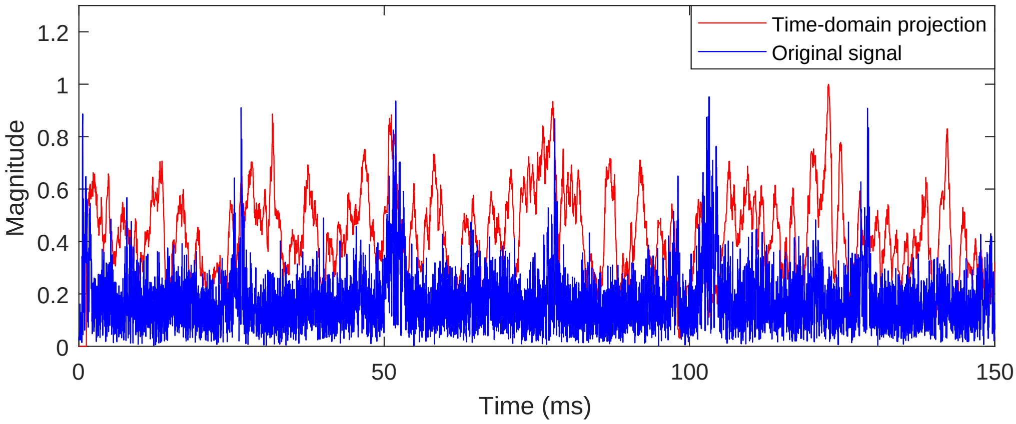

(a) Using $n_s = 2.5ms$

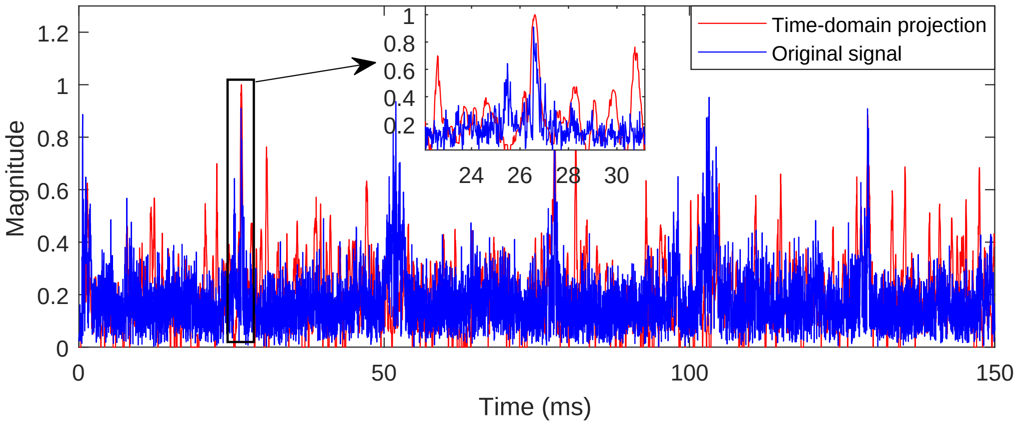

(b) Using $n_s = 0.6ms$

Figure 9: The original signal (no noise) and time-domain Radon transform projected signal with a $SNR = -18dB$ for the Squirrel helicopter measured at 0° aspect.

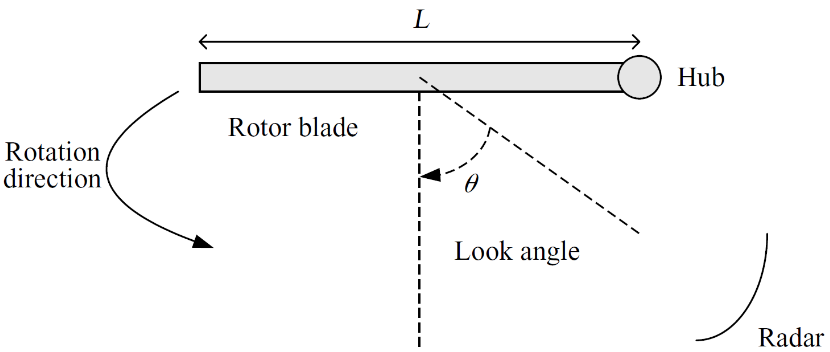

Figure 10: Look angle geometry [1].

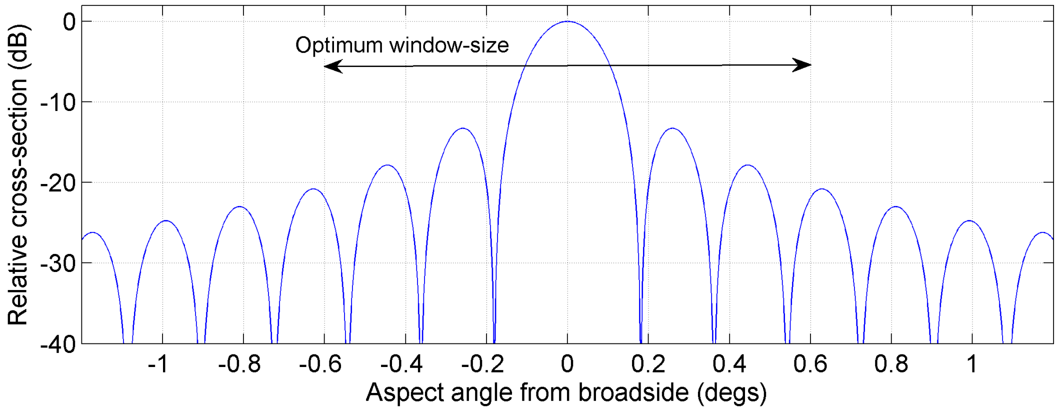

Figure 11: The modelled RCS of the main rotor blade of the Bell helicopter with look angle θ, where the radar carrier frequency is 9.5 GHz and the length of the main blade is $L = 5$ m. The optimum window length is shown here as having an angular extent of approximately $1.2°$.

Table 1: The main blade detection parameters for CPIs of 50 and 75 ms, estimated for positive and negative spectra blade flashes, for a hovering Bell helicopter at 180° aspect, using $n_s = 0.5$ ms.

	CPI = 50 ms		**CPI = 75 ms**	
	+ ve	- ve	+ ve	- ve
Q-factor	0.5	0.5	0.5	0.5
τ (ms)	38.7	39.1	38.6	39.0

Table 2 presents the main blade measured Q-factor and time values (τ) for approaching and receding blades (±ve) for varying CPI values for the Squirrel helicopter. For main blade detection, the estimated Q-factor for the approaching and receding blades using a CPI of 50 ms is 0.9 and 0.58 respectively. This is below the Q-factor detection threshold of 1.5 and hence a main blade is detected on both sides of the spectrum. The maximum blade flashes were detected at 0.2 ms and 26.6 ms for the approaching and receding blades respectively, and correspond with the flashes seen in the STFT plot in Figure 1b.

Using a CPI of 100 ms, the maximum main blade flashes were detected at 51.8 ms and 26.4 ms respectively. The flash detected on the positive side of the spectrum is different but still gives

Table 2: The main blade detection parameters for CPIs of 50 and 75 ms, estimated for positive and negative spectra blade flashes, for a hovering Squirrel helicopter at 0° aspect, using $n_s = 0.9$ ms.

	CPI = 50 ms		**CPI = 100 ms**	
	+ ve	- ve	+ ve	- ve
Q-factor	0.90	0.58	0.77	0.58
τ (ms)	0.20	26.6	51.8	26.4

a Q-factor of 0.77. Again, the Q-factors for this CPI are below the detection threshold of 1.5 and hence a main blade is detected on both sides of the spectrum.

Overall, we observe that the detection algorithm, using the STFT window-size within the optimal range as discussed in Section 3.1, still works using shorter CPIs. This makes sense because the algorithm assumes at least one blade flash is present in the data and only considers the blade flash with the maximum reflectivity. Hence *the only requirement on CPI length is that it should be long enough to capture at least a single blade flash during the CPI.* The performance of the detection algorithm is not affected by CPI but the reflectivity of the blade flash during the CPI. Conceivably, for very short CPIs where no main blade flash occurs, helicopter detection can occur using the tail blade. A more detailed discussion about this is reserved for Section 4.

3.3. Impact of Overlap Factor

In this section we investigate the impact of the overlap factor on the algorithm performance. In the STFT, the overlap factor is as illustrated in Figure 12. It characterises the redundancy factor of the transform. Here, the overlap factor is stated as a percentage of the STFT window-size, where an overlap factor of 50% means the each segment overlaps by half n_s, and the highest redundancy factor of a STFT is obtained when overlap size is equal to $n_s - 1$, or close to 100% overlap. Setting a high redundancy factor ensures the STFT captures all the significant features in the original time domain, where as, a very low redundancy factor will result in a mismatch between the basis functions and the blade returns. Thus, the resultant energy in STFT domain will reduce potentially causing mis-detections when competing with high noise. Figure 13 shows the detection performance as a function of STFT window-size for the 50% and maximum overlap cases.

Overall there is a small positive impact on the detection performance using the maximum overlap. The optimal STFT window-size for both cases is still in the range of $0.5-1.0$ ms which is consistent with the results presented in Section 3.1. However, the detection performance has improved for small STFT window-sizes making the choice of a small window-size less critical. There is however an increase in computational time as a result of the increased overlap factor, which can be significant for long CPIs. Compared to the STFT window-size, the overlap factor has minimal impact on the proposed blade flash detection algorithm.

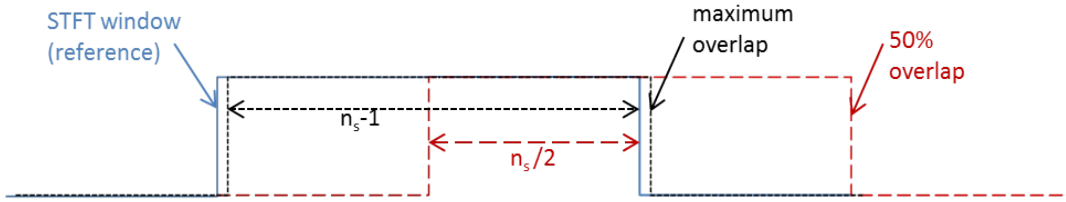

Figure 12: Illustration of STFT window overlap factor.

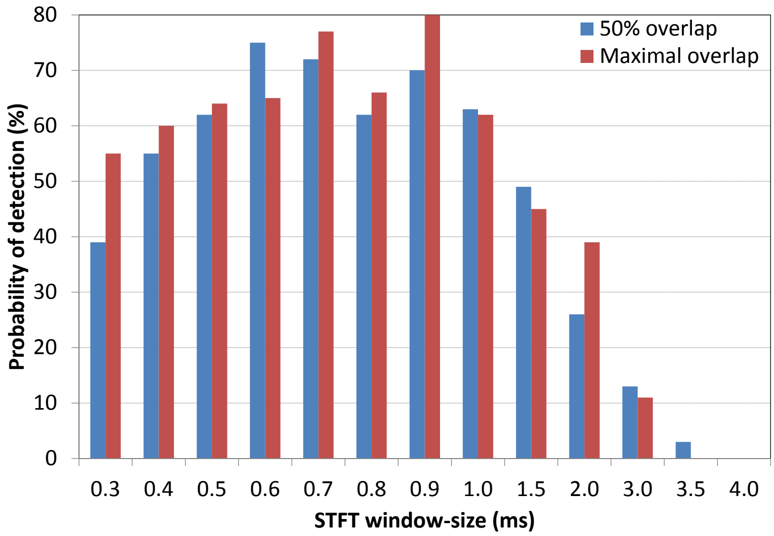

Figure 13: The probability of detection versus the STFT window-size for a hovering Squirrel helicopter at 0° aspect, with SNR = -18 dB, for two different values of the overlap factor. The maximum overlap factor varies from 95% to 99% as the STFT window-size changes from 0.3 ms to 4 ms.

3.4. Discussion

Using the two datasets, we have demonstrated that among all the STFT parameters, the performance of blade flash signal detection algorithms is most significantly affected by the STFT window-size. For both the Bell and Squirrel helicopters, we observe a similar trend in the algorithm detection performance, with the best detection performances occurring for STFT window-sizes in the range of 0.5 ms to 1.0 ms. Specifically, for the best detection performance results, the optimum window-size for the Bell and Squirrel helicopters were 0.5 ms and 0.6 ms respectively, which corresponds to the time-domain blade flash duration. Also, with this dataset, the Q-factor threshold is set to 1.5, however, it should be noted that this value may vary for helicopters with different blade lengths and rotation rates. This is still to be investigated and is reserved for future work.

The CPI length has little effect on the detection performance, but affects the number of main and tail blade flashes occurring during the CPI. With longer CPIs, the variability in blade reflectivity over time means the probability of capturing a blade flash having a strong return is more likely and hence competition with noise is reduced. This should be considered in conjunction with the overlap factor which produced slightly improved detection performance but with increased computational time which is compounded by long CPIs. A compromise between the two is needed and will depend on the application. For radar systems where time on target is low, increasing the overlap factor may have some benefit, however, for long dwell times, capturing the variability in blade reflectivity over time may prove better in low SNR conditions.

As expected, aspect angle of the helicopter with respect to the radar has a significant impact on the probability of detection. As shown in Figure 7, at 0° aspect the target SNR range where P_d varies approximately between 0 and 1 is $(-24, -12)$ dB. On the other hand, when the helicopter aspect is 180° this SNR range reduces to $(-30, -16)$ dB as shown in Figure 4. In its current form, the proposed algorithm is unable to detect multiple helicopter targets. As it relies on the dominant blade flash, it will detect the helicopter with the dominant return but cannot confirm the presence of multiple helicopters. Depending on the spatial separation of two helicopters compared to radar's range and azimuth resolutions, they may be separated in range or angle.

4. Tail Blade Detection

The aim of this section is to present results on the detection of the tail blade component in the signal after the main blade component has been correctly extracted. The blade flash extraction algorithm was discussed in [7] using a compressive sensing approach which showed that effective separation/extraction of the blade flash component can be obtained. The algorithm first requires a detection and declaration of the strongest blade flash component, from which the algorithm parameter is computed, followed by the blade extraction routine using the computed parameters. After the extraction is executed, it will continue to extract other blade flash components, if any exists.

However, whilst detection and extraction of the main blade was effective, it was reported to encounter issues with detection of the low SNR tail blade signals. It should be noted that detection and extraction of both blades rotors provide extra information for automatic target recognition (ATR). That is, if both main and tail blades can be detected, information about the number of rotors will be known. In addition, if both main and tail components can be effectively extracted, from which the number of main and tail blades can be computed and thus the associated rotation rates, then this information can be critical for ATR [18]. The Bell and Squirrel helicopter datasets used in the previous section will be used to demonstrate tail detection.

For this investigation, STFT window sizes of $n_s = 2.5$ ms and $n_s = 1.0$ ms will be used for the Bell dataset, and window sizes of $n_s = 2.5$ ms and $n_s = 0.9$ ms will be used for the Squirrel dataset. These sub-optimum values were chosen to highlight the impact of window-size on the resulting STFT and detection performance and to present typical Q-factor values that fall outside the detection threshold.

The estimated Q-factor and τ parameters for the Bell helicopter is summarised in Table 3. For $n_s = 2.5$ ms the estimated Q-factor for the positive and negative sides of the spectrum were 4.5 and 2.1, respectively. These are larger than the Q-factor threshold of 1.5 so no detection is declared and hence no τ values are found. Figure 14a shows the STFT of the signal after the main blade component is removed. Although the tail returns are visibly discernible, especially on the negative side of the spectrum, the temporal broadening of the tail blade flashes has caused a mis-detection.

For n_s=1.0 ms the estimated Q-factor for the positive and negative sides of the spectrum were 1.16 and 0.9 respectively. With these Q-factors a detection is declared and the τ values

Table 3: The estimated parameters for positive and negative spectrum blade flashes for a hovering Bell helicopter at 180° aspect.

	n_s = **2.5 ms**		n_s = **1.0 ms**	
	+ve	-ve	+ve	-ve
Q-factor	4.50	2.10	1.16	0.90
τ (ms)	-	-	97.3	11.8

are estimated at 97.3 ms and 11.8 ms for the positive and negative sides of the spectrum respectively. Figure 14b shows the STFT of the signal after the main blade is extracted and indicates the temporal positions of the detected blades. Again the tail returns are visibly discernible with less temporal broadening of the blade flash. Also, the tail blade flash on the positive side of the spectrum (indicated by the arrow at 97.3 ms) has been detected. These two cases highlight further the dependence of window-size on detection performance.

For the Squirrel helicopter the estimated Q-factor and τ parameters are summarised in Table 4. For $n_s = 2.5$ ms the estimated Q-factor for the positive and negative sides of the spectrum are 0.89 and 1.61 respectively. This means that tail detection is declared on the positive side of the spectrum only which can be confirmed by looking at the spectrogram in Figure 15a.

Similar to the case of the Bell helicopter, reducing the STFT window-size to 0.9 ms enables the detection of the low-level tail blade returns where the estimated Q-factor for the positive and negative sides of the spectrum are 0.76 and 0.77 respectively. Figure 15b shows the STFT of the signal after the main blade component is removed and indicates the temporal positions of the detected blades at 83.3 ms and 156.4 ms.

Table 4: The estimated parameters for positive and negative spectrum blade flashes of the Squirrel helicopter at 0° aspect.

	n_s = **2.5 ms**		n_s = **0.9 ms**	
	+ve	-ve	+ve	-ve
Q-factor	0.89	1.61	0.76	0.77
τ (ms)	98.1	-	83.3	156.4

For the two helicopter cases presented here, we have demonstrated that the proposed algorithm performs well for detecting blade-like components in the signal. Although the detection of the tail blade is secondary to the main blade detection, it provides confirmation of a helicopter target and provides an alternative feature to detect in the absence of main blade components in the signal with a short CPI. Similar to the main blade, future studies will investigate the optimal parameters for improving the detection of the tail blade of the helicopter in a low SNR environment.

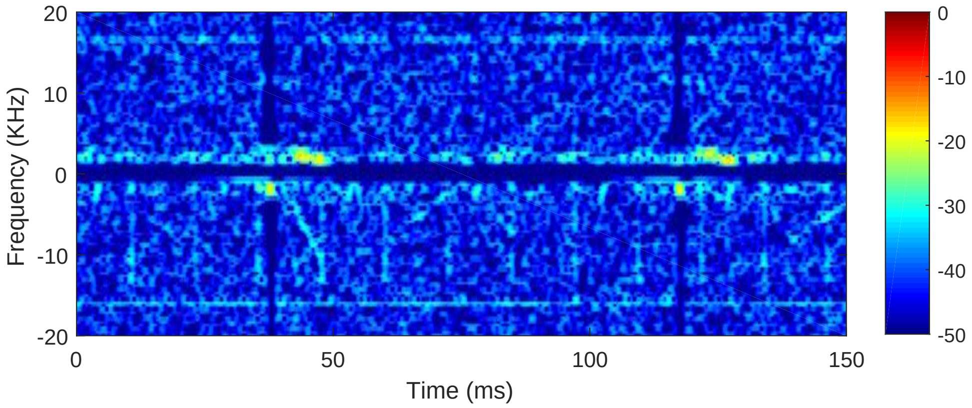

(a) $n_s = 2.5\ ms$

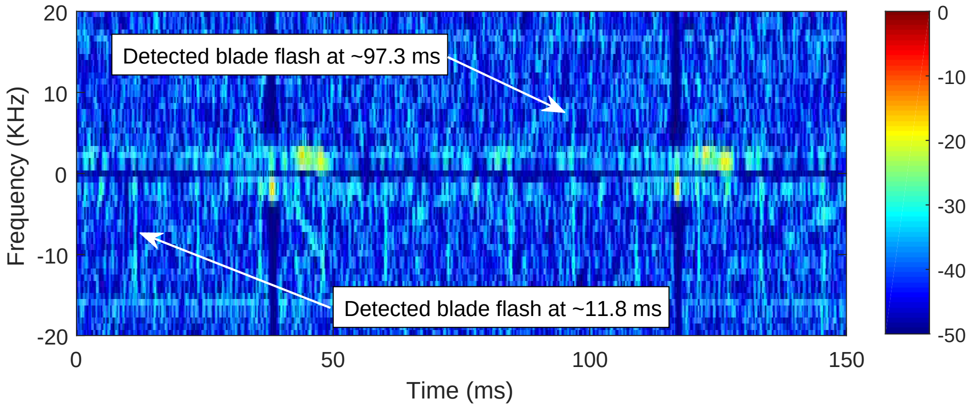

(b) $n_s = 1.0\ ms$

Figure 14: STFT plot of the remnant signals after main blade extraction for the hovering Bell helicopter at 180° aspect, for varying n_s values.

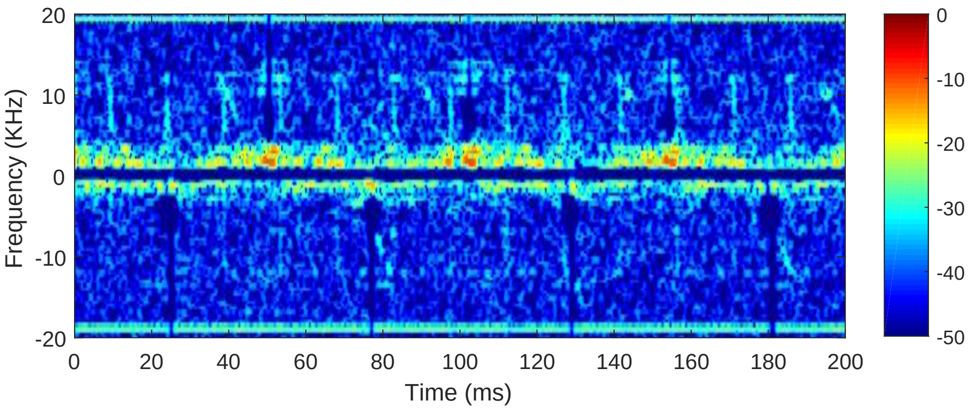

(a) $n_s = 2.5\ ms$

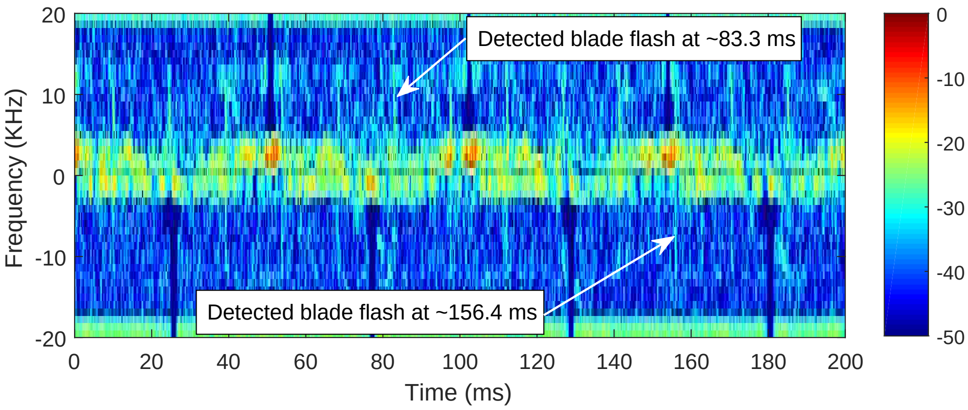

(b) $n_s = 0.9\ ms$

Figure 15: STFT plot of the remnant signals after first extraction for the hovering Squirrel helicopter at 0° aspect, for varying n_s values.

5. Concluding Remarks

We have evaluated the performance of our blade flash detection algorithm in low SNR conditions, and investigated the impact of various parameters, such as STFT window-size, CPI and overlap factor, on the algorithm's performance. The case studies in this report highlight the fact that tuning the critical parameters of the proposed algorithm is essential in improving the detection performance of the helicopter's blade returns in low SNR conditions. Results show that all the STFT parameters and radar parameters influence performance of the blade detection algorithm. However, the STFT window-size has the most significant impact on the detection performance of the algorithm and should be matched to the duration of the blade flashes.

Acknowledgements

This work was successfully undertaken under Collaborative Project Agreement (ID: 6712) between DST Group and the University of Adelaide. The authors would like to thank Dr. Leigh Powis and Dr. Jonathan Legg for critically reviewing the report and providing useful comments.

6. References

[1] Tait, P. (2005) *Introduction to Radar Target Recognition*, Vol. 18, IET.

[2] Chen, V. C., Li, F., Ho, S.-S. & Wechsler, H. (2006) Micro-Doppler effect in radar: phenomenon, model, and simulation study, *IEEE Transactions on Aerospace and Electronic Systems* **42**(1), 2–21.

[3] Tikkinen, J., Hiltunen, K., Martikainen, K. & Isohookana, M. (2012) Helicopter Detection Capability of Passive Coherent Location (PCL) Radar, *in Proceedings of the 9th European Radar Conference*, pp. 138–141.

[4] Misiurewicz, J., Kulpa, K. & Czekala, Z. (1998) Analysis of radar echo from a helicopter rotor hub, *in 12th International Conference on Microwaves and Radar*, pp. 866–870.

[5] Nguyen, S. T. N., Kodituwakku, S., Melino, R. & Tran, H. T. (2017) Wavelet-based Sparse Representation for Helicopter Main Rotor Blade Radar Backscatter Signal Separation, *IEEE Transactions on Aerospace and Electronic Systems* **53**(6), 2936–2949.

[6] Nguyen, S. T. N., Kodituwakku, S., Melino, R. & Tran, H.-T. (2016) Signal Separation Of Helicopter Radar Returns Using Wavelet-Based Sparse Signal Optimisation, *DST-Group-RR-0436*.

[7] Nguyen, S. T. N., Melino, R., Tran, H.-T. & Kodituwakku, S. (2017) Automatic Helicopter Blade Flash Signal Separation Using Sparse Signal Optimisation, *DST-Group-RR-0442*.

[8] Misiurewicz, J., Kulpa, K., Czekala, Z. & Filipek, T. (2012) Radar Detection of Helicopters with Application of CLEAN Method, *IEEE Transactions on Aerospace and Electronic Systems* **48**(4), 3525–3537.

[9] Xie, Y.-A., Tao, R., Miao, H.-X. & Ma, J.-M. (2016) The helicopter target detection based on micro-Doppler analysis and implementation, *in 35th Chinese Control Conference*, pp. 5143–5148.

[10] Haghshenas, H. & Nayebi, M. M. (2010) A novel method to detect rotor blades echo, *in IEEE Radar Conference*, pp. 1331–1334.

[11] Gini, F. & Farina, A. (1999) Matched subspace CFAR detection of hovering helicopters, *IEEE transactions on Aerospace and Electronic Systems* **35**(4), 1293–1305.

[12] van Koersel, A. C. (2000) Helicopter detection and classification demonstrator, *in Proceedings of SPIE*, Vol. 4040.

[13] Raju Damarla, T. & Ufford, D. (2008) Helicopter detection using harmonics and seismic-acoustic coupling, *in Proceedings of SPIE, the International Society for Optical Engi-*

neering, Vol. 6963.

[14] Akhtar, S., Elshafei-Abmed, M. & Ahmed, M. S. (2001) Detection of helicopters using neural nets, *IEEE Transactions on Instrumentation and Measurement* **50**(3), 749–756.

[15] Sadati, N. & Faghihi, A. (2006) Neural networks in identification of helicopters using passive sensors, *in IEEE International Conference on Systems, Man and Cybernetics*, pp. 7–10.

[16] Zhang, Q., Yeo, T. S., Tan, H. S. & Luo, Y. (2008) Imaging of a moving target with rotating parts based on the Hough transform, *IEEE Transactions on Geoscience and Remote Sensing* **46**(1), 291–299.

[17] Luo, Y., Zhang, Q., Qiu, C.-w., Liang, X.-j. & Li, K.-m. (2010) Micro-Doppler effect analysis and feature extraction in ISAR imaging with stepped-frequency chirp signals, *IEEE Transactions on Geoscience and Remote Sensing* **48**(4), 2087–2098.

[18] Gaglione, D., Clemente, C., Coutts, F., Li, G. & Soraghan, J. J. (2015) Model-based sparse recovery method for automatic classification of helicopters, *in IEEE Radar Conference (RadarCon)*, IEEE, pp. 1161–1165.

DEFENCE SCIENCE AND TECHNOLOGY GROUP DOCUMENT CONTROL DATA						1. DLM/CAVEAT (OF DOCUMENT)
2. TITLE Radar Detection of Helicopters at low SNR using Time-Frequency Transforms			3. SECURITY CLASSIFICATION (FOR UNCLASSIFIED LIMITED RELEASE USE (L) NEXT TO DOCUMENT CLASSIFICATION) Document (U) Title (U) Abstract (U)			
4. AUTHORS Duong Duc Nguyen, Si Tran Nguyen Nguyen, Rocco Melino, Sandun Kodituwakku and Hai-Tan Tran			5. CORPORATE AUTHOR Defence Science and Technology Group PO Box 1500 Edinburgh, South Australia 5111, Australia			
6a. DST GROUP NUMBER DST-Group–TR–3481	6b. AR NUMBER 017-169		6c. TYPE OF REPORT Technical Report		7. DOCUMENT DATE April, 2018	
8. OBJECTIVE ID		9. TASK NUMBER N/A		10. TASK SPONSOR N/A		
11. MSTC Surveillance and Reconnaissance Systems			12. STC Surveillance Modelling and Analysis			
13. DOWNGRADING/DELIMITING INSTRUCTIONS `http://dspace.dsto.defence.gov.au/dspace/`			14. RELEASE AUTHORITY Chief, National Security and ISR Division			
15. SECONDARY RELEASE STATEMENT OF THIS DOCUMENT *Approved for Public Release* OVERSEAS ENQUIRIES OUTSIDE STATED LIMITATIONS SHOULD BE REFERRED THROUGH DOCUMENT EXCHANGE, PO BOX 1500, EDINBURGH, SA 5111						
16. DELIBERATE ANNOUNCEMENT No Limitations						
17. CITATION IN OTHER DOCUMENTS No Limitations						
18. RESEARCH LIBRARY THESAURUS Helicopter detection, Short-Time Fourier Transform, Micro-Doppler						
19. ABSTRACT This report describes a radar signal processing technique for detecting helicopter targets based on the micro-Doppler components of the received signal, in a low SNR environment. The Short-Time Fourier Transform (STFT) and the tunable Q-factor wavelet transform were used to identify the micro-Doppler components induced from the rotating main and tail rotor blades of a helicopter radar return. The impact of the STFT parameters on identifying the blade-like components in the reflected signal was investigated. A strong correlation exists between the STFT parameters and the physical properties of the main and tail rotor blades, which can be used to tune the algorithm and improve the detection performance. The algorithms proposed are demonstrated using measured radar data from two different helicopter types.						